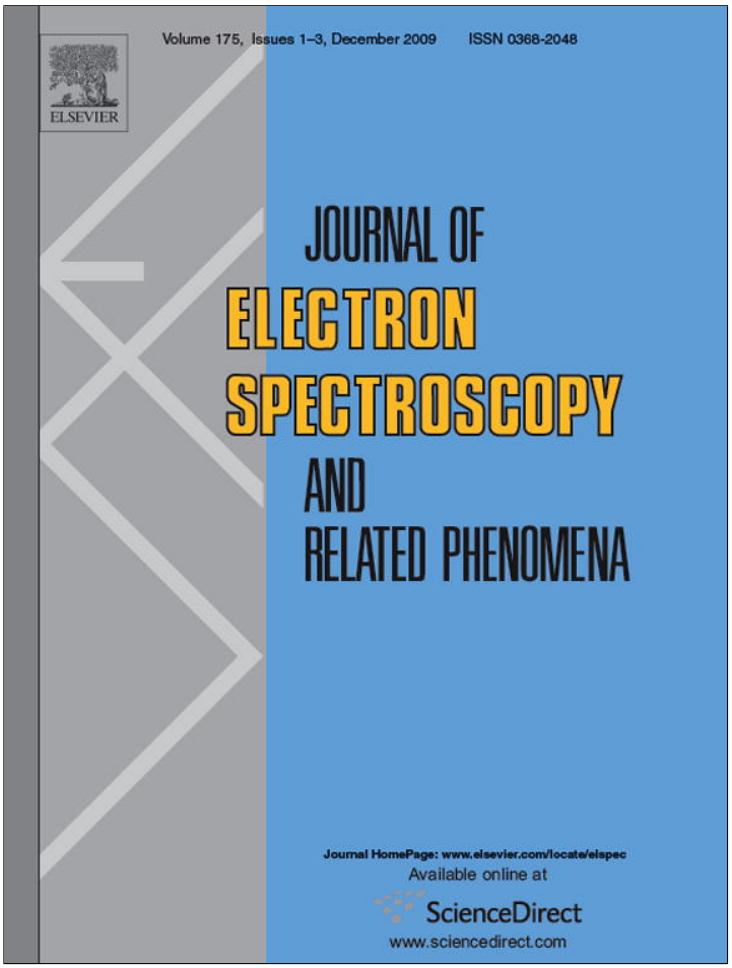

Journal of Electron Spectroscopy and Related Phenomena 175 (2009) 21–26

Contents lists available at ScienceDirect

Journal of Electron Spectroscopy and Related Phenomena

journal homepage: www.elsevier.com/locate/elspec

XPS and magnetic studies of vanadium tellurite glassses

A. Mekki[a,*], G.D. Khattak[a], L.E. Wenger[b]

[a] Physics Department, King Fahd University of Petroleum & Minerals, Dhahran 31261, Saudi Arabia
[b] Department of Physics, The University of Alabama at Birmingham, Birmingham, AL 35294-1170, USA

ARTICLE INFO

Article history:
Received 28 February 2009
Received in revised form 4 July 2009
Accepted 5 July 2009
Available online 18 August 2009

Keywords:
Vanadium tellurite glasses
XPS study of vanadate glasses
Magnetic susceptibility of vanadate glasses

ABSTRACT

A series of tellurite glasses containing vanadium with nominal composition xV_2O_5–$(1-x)TeO_2$, where $x = 0.1$, 0.2, 0.3, and 0.4, have been prepared by melt quenching technique and investigated using X-ray photoelectron spectroscopy (XPS) and magnetization techniques. The Te 3d core level spectra show asymmetry and therefore were fitted with two contributions one from Te ions in TeO_4 trigonal bipyramid (tbp) configuration and the other from Te ions in TeO_3 trigonal pyramid (tp) configuration. Quantitative analysis of the areas of both components support the model of a change of TeO_4 tbp to TeO_3 tp upon V_2O_5 addition. The V 2p core level spectra did not show any asymmetry and were fitted with a single component corresponding to V^{5+} while the O 1s core level spectra show slight asymmetry on the higher binding energy side of the main peak and were fitted with two contributions, one due to bridging oxygen (BO) atoms and the other due to non-bridging oxygen (NBO) atoms. The fraction of NBO, determined from these spectra, is found to increase with increasing V_2O_5 content suggesting the formation of TeO_3 units and also that V_2O_5 is acting as a glass modifier in this glass series. The magnetic susceptibility data for these glasses follow a Curie–Weiss behavior ($M/H = C/(T-\theta)$) which also indicates the presence of some V ions existing in a magnetic state, i.e., a valence state other than that of the non-magnetic state V^{5+}. The ratios of V^{4+}/V_{total} as determined from magnetic susceptibility measurements assuming only the presence of magnetic V^{4+} and non-magnetic V^{5+} ions vary from 0.030 to 0.037. These ratios are too small to be detected by XPS measurements and this is why no asymmetry is observed in the V2p spectra of these glasses.

1. Introduction

Tellurite glasses are high-index optical glasses that permit high levels of infrared radiation to be transmitted and thus have potential applicability as materials for acousto-optical devices and lasers, or as photochromic glasses. Tellurium dioxide, like vanadium pentoxide, is a conditional glass former and is the basis for forming the tellurite glasses. From various spectroscopic methods such as infrared [1–3], Raman [3–7], nuclear magnetic resonance [8], and X-ray absorption spectroscopy [9–11] as well as from X-ray [11,12] and neutron diffraction [13,14] techniques, it has been established that the basic structure of the tellurite glasses is a TeO_4 trigonal bipyramid (tbp) with a lone pair of electrons in one of its equatorial sites. Tellurium oxide under normal conditions does not have the ability to form a glass structure easily without a modifier like an alkali oxide, an alkaline-earth oxide, a transition-metal oxide, or another glass former [13,15]. Researchers have different opinions as to why it is so difficult to form a glass of pure TeO_2. Neov et al. [13,15] hypothesized that TeO_2 could not form a glass by itself because the Te–O bond is too strongly covalent to permit the requisite amount of distortion for a glass structure. Another prevalent view [16,17] is that the repulsive forces due to the lone pair of electrons resist the free movement of the trigonal bipyramid in space during the cooling of the melt and hence the formation of glass. In a binary tellurite glass the effect of the lone pair of electrons is limited by the introduction of new structural units that are compatible with TeO_4 (tbp) and thus the glass formation becomes easier.

The addition of another conditional glass former such as V_2O_5 to TeO_2 has been extensively studied by several authors. For example, Sakida et al. [18] studied the structure of V_2O_5–TeO_2 glasses by means of ^{125}Te and ^{51}V static NMR spectroscopies. They found that the fraction of TeO_3 and the NBO sites increase with increasing V_2O_5 content. Hoppe et al. [19] used neutron diffraction to study the structure of this glass system. They found that in glasses of 10 mol% V_2O_5 each VO_n polyhedron is accompanied with a TeO_3 unit. The number of TeO_3 units increases further for glasses of higher V_2O_5 fractions but it remains less than the number of V sites. The results are largely in agreement with those of Sakida et al. However, both authors did not estimate the fraction of various oxidation states in the glasses.

X-ray photoelectron spectroscopy (XPS) has been found to be a useful technique in assessing the local glass structure and even

* Corresponding author. Tel.: +966 38604292; fax: +966 38602293.
E-mail address: akmekki@kfupm.edu.sa (A. Mekki).

0368-2048/$ – see front matter © 2009 Elsevier B.V. All rights reserved.
doi:10.1016/j.elspec.2009.07.001

Table 1
Nominal and actual composition (molar fraction) of xV_2O_5–$(1-x)TeO_2$.

Nominal		Actual (from ICP)	
V_2O_5	TeO_2	V_2O_5	TeO_2
0.10	0.90	0.09	0.91
0.20	0.80	0.18	0.82
0.30	0.70	0.27	0.73
0.40	0.60	0.36	0.64

The relative uncertainty in the ICP results is ±5%.

estimating the ratio of the different valence states in the TM-oxide glasses [20]. In this study, the state of V ions in vanadium-tellurite glasses will be presented from XPS spectra in combination with magnetization measurement data. We will also use XPS to measure the NBO and TeO_3 content in these glasses and compare our findings with those of previous work.

2. Experimental procedure

2.1. Glass preparation

All glasses were prepared by melting dry mixtures of reagent grade V_2O_5 and TeO_2 in alumina crucibles to form batch xV_2O_5–$(1-x)TeO_2$ compositions with $x = 0.1, 0.2, 0.3$, and 0.4. Since oxidation and reduction reactions in a glass melt are known to depend on the size of the melt, on the sample geometry, on whether the melt is static or stirred, on thermal history, and on quenching rate, all glass samples were prepared under similar conditions to minimize these factors. Approximately 30 g of chemicals were thoroughly mixed to obtain a homogenized mixture for each V_2O_5 concentration. The crucible containing the batch mixture was then placed electrically heated melting furnace maintained at 850–900 °C. The melt was left for about 1 h under atmospheric conditions in the furnace during which the melt was occasionally stirred with an alumina rod. The homogenized melt was then cast onto a stainless steel plate mold to form glass buttons and glass rods of approximately 5-mm diameter for XPS measurements. X-ray powder diffraction analysis indicated that the glasses formed were completely amorphous. After preparation, the samples were stored in a vacuum dessicator to minimize any further oxidation of the glass samples. The actual compositions of the glasses were determined by inductively coupled plasma spectroscopy (ICP) and are listed in Table 1. Although the inclusion of alumina from the crucibles used in the melting of the glass mixtures is a possible source of impurities, no signals for aluminum were detected in both the XPS and ICP studies of these glasses.

2.2. X-ray photoelectron spectroscopy (XPS)

High-resolution photoelectron spectra were collected on a VG scientific ESCALAB MKII spectrometer equipped with dual aluminium–magnesium anode using Al K(radiation ($h\nu = 1486.6$ eV). The electron analyzer was set at a pass energy of 20 eV. The energy scale of the spectrometer was calibrated using the core level of Cu $2p_{3/2}$ (932.4 eV) and the energy separation between Cu $2p_{3/2}$ and Cu $2p_{1/2}$ (19.8 eV). For self-consistency, the C 1s line of 284.6 eV binding energy was used as a reference for all charge shift corrections as this peak arises from hydrocarbon contamination and its binding energy is generally accepted as remaining constant, irrespective of the chemical state of the sample. This hydrocarbon contamination was further enhanced as the XPS measurements had to be performed on uncleaved surfaces of the glasses as the glass rod samples shattered under vacuum cleavage. The typical time required to collect an XPS spectrum for a sample was about 4 h and the base pressure in the analysis chamber during these measurements was less than 10^{-10} mbar.

2.3. Magnetization measurements

Temperature-dependent dc magnetic susceptibilities were measured using a Quantum Design SQUID magnetometer (model MPMS-5S) in a magnetic field of 5000 Oe over a temperature range of 5–300 K. Each glass sample was suspended by thread in order to eliminate any sample holder correction to the measured magnetization. The overall accuracy of the magnetic measurements is estimated to be approximately 3% due to the uncertainty of the magnetometer calibration.

3. Results

Fig. 1 shows high resolution Te 3d spin-orbit doublet spectra for the tellurite containing glasses. The peak intensity decreases with increasing V_2O_5 content in the glasses, while the peak position for Te $3d_{5/2}$ at ~576.5 eV does not vary much with composition. The peak width at half maximum (FWHM) shows first an increase, then a decrease with increasing V_2O_5 content. This variation might indicate the change of TeO_4 tbp to TeO_3 tp configuration with the addition of V_2O_5 content. The O 1s core level spectra are displayed in Fig. 2 for all compositions. A slight asymmetry is observed on the higher binding energy (BE) side of the main peak having an average value of ~530.5 eV. This peak is also fitted with two contributions, one due to oxygen atoms in a bridging environment (BO) and the other due to oxygen atoms in a non-bridging environment (NBO). The O 1s spectra show an increase in intensity and this is well understood since we are substituting TeO_2 by V_2O_5 and therefore introducing more oxygen atoms with increasing V_2O_5 content in the glass. Fig. 3 shows the V 2p spin-orbit doublet. The peak intensity of the V $2p_{3/2}$ increases with increasing V_2O_5 content in the glass but its BE does not vary much and has an average value of ~517.2 eV. The full-width at half maximum (FWHM) is also constant at ~1.9 eV for all glasses. This indicates that vanadium ions might exist mostly in a single oxidation state.

The temperature dependence of the magnetic susceptibility data for all glass samples appear to follow a Curie–Weiss behavior, $M/H = C/(T-\theta)$, with a temperature-independent background. After determining the background contribution from a high-temperature extrapolation of M/H-vs-$1/T$ plots, the resulting M_{corr}/H ($=M/H-(M/H)_{background}$) data were found to follow a Curie–Weiss behavior, $M_{corr}/H = C/(T-\theta)$, with the Curie constant

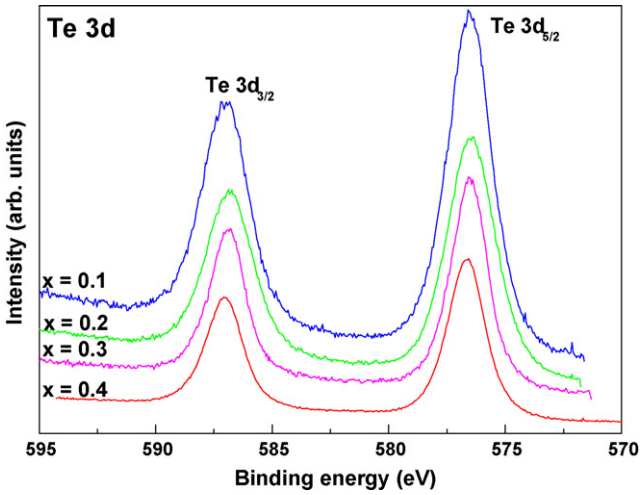

Fig. 1. Te 3d core level spectra for the vanadium tellurite glasses.

Table 2
Magnetic susceptibility results for the copper telluride xV_2O_5–$(1-x)TeO_2$ glasses and the concentration of V^{4+} ions to total vanadium ions.

x	$(M/H)_{background}$ (10^{-7} emu/Oe g)	C (10^{-5} emu K/Oe g)	θ (K)	$[V^{4+}]/[V_{total}]$
0.10	−2.23	1.39	1.06	0.030
0.20	−2.05	3.08	−0.05	0.034
0.30	−0.71	5.22	1.24	0.039
0.40	−0.26	6.62	0.57	0.037

Table 3
Peak positions (in eV) for the core levels Te 3d, V 2p and O 1s relative to C 1s (284.6 eV), their corresponding full-width at half maximum (FWHM) and separation ΔE of the spin orbit peaks xV_2O_5–$(1-x)TeO_2$ glasses.

x	Te $3d_{5/2}$ FWHM (eV)	ΔE Te 3d (eV)	V $2p_{3/2}$ FWHM (eV)	ΔE V 2p (eV)	O 1s FWHM (eV)
0.10	576.5	10.6	517.1	7.3	530.4
	2.45		2.0		2.5
0.20	576.5	10.4	517.1	7.3	530.5
	2.61		2.0		2.5
0.30	576.6	10.3	517.2	7.3	530.6
	2.11		1.8		1.9
0.40	576.7	10.4	517.3	7.3	530.6
	2.13		1.8		2.0
TeO_2	576.1	10.4			530.3
	2.1				1.93
V_2O_5			517.3	7.3	530.2
			2.0		1.89

The uncertainty in the peak position is ±0.10 eV and in FWHM is ±0.20 eV.

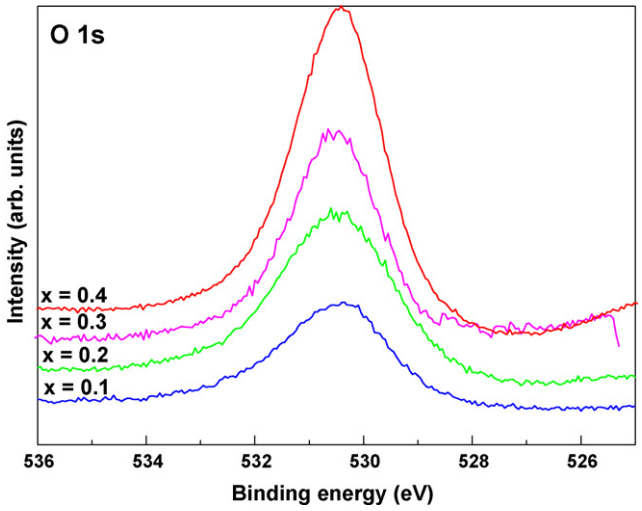

Fig. 2. O 1s core level spectra for the vanadium tellurite glasses.

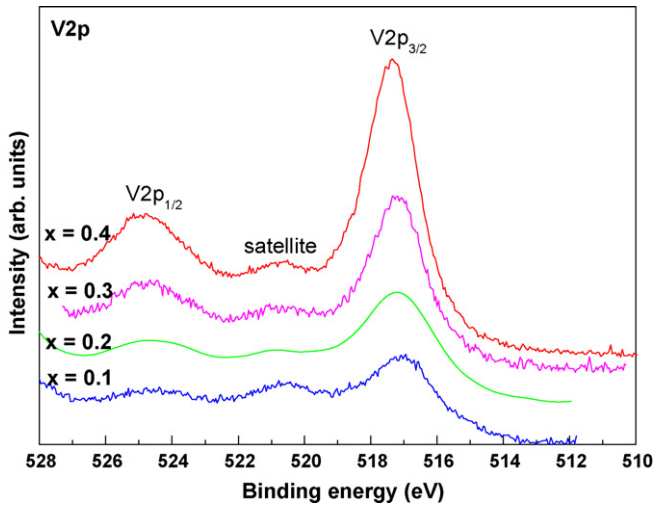

Fig. 3. V 2p core level spectra for the vanadium tellurite glasses.

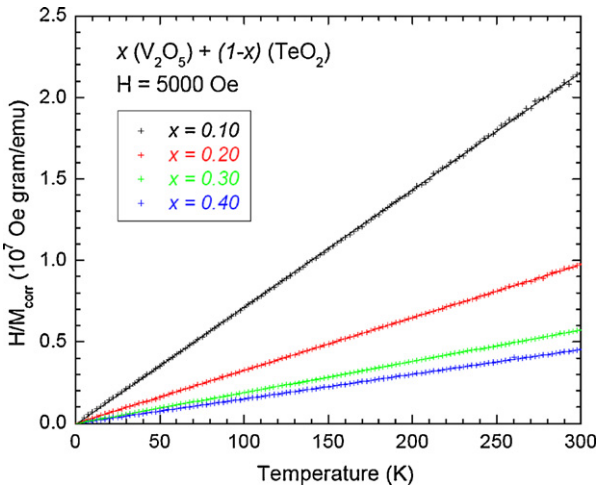

Fig. 4. The inverse of the "corrected" magnetic susceptibility M_{corr}/H $(=M/H - M_{background}/H)$ as a function of the temperature T for the vanadium tellurite glasses.

C and the paramagnetic Curie temperature θ determined from the least-squares fits of the H/M_{corr}-vs-T data as shown in Fig. 4. Table 2 displays these parameters ($(M/H)_{background}$, C, and θ) for each of the glass samples. From the Curie constant C, the relative fraction of V^{4+} ($\mu_{eff} = 1.8\ \mu_B$) was determined assuming that only V^{4+} and V^{5+} ($\mu_{eff} = 0\ \mu_B$) ions were present in these glasses.

4. Discussion

Although vanadium can exist in two oxidation states V^{4+} and V^{5+} in glasses but the observation that the peak position and the width of the V $2p_{3/2}$ peak do not change much with the V_2O_5 content in these glasses (see Table 3) suggests that vanadium ions probably exists in only one oxidation state. In a previous study on vanadium phosphate glasses [21] it was found that the core level spectrum of V^{5+} has a $2p_{3/2}$ BE of ~517.3 eV, while that of V^{4+} is at a BE of ~516.1 eV. Thus fitting the V $2p_{3/2}$ core level peak into two contributions, one from the V^{4+} ions at a BE of ~516 eV and the other

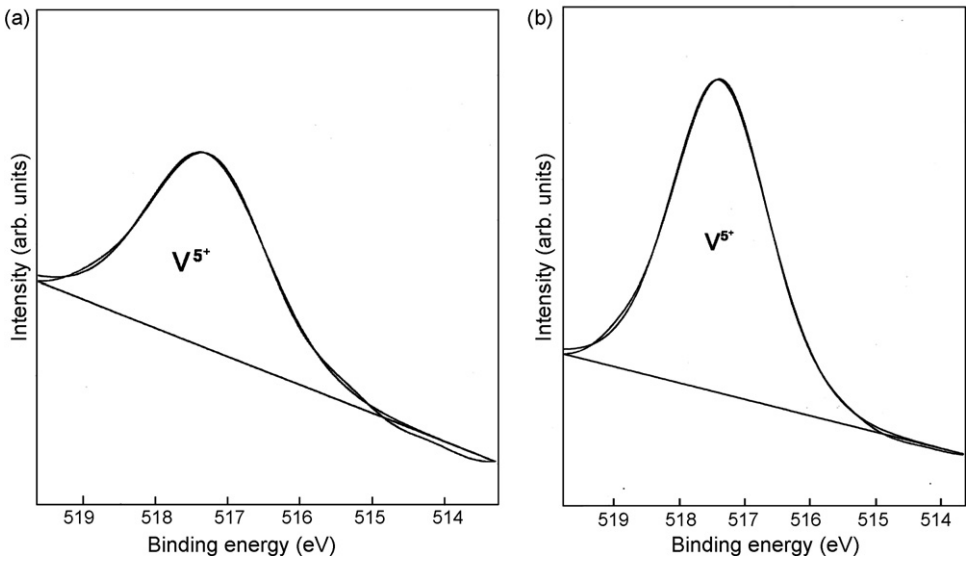

Fig. 5. V $2p_{3/2}$ core level spectra fitted with a single peak due to V^{5+} for (a) $x = 0.1$ and (b) $x = 0.4$ glass compositions.

due to V^{5+} ions at a BE of ~517.3 eV, should permit a more quantitative estimate of the relative V concentration for these two oxidation states of vanadium. The sum of two weighted Gaussian–Lorentzian peaks centered at approximately 516 and 517.3 eV is then fitted to the experimental data. It is clear from Fig. 5 that the V $2p_{3/2}$ core level spectra for the $x = 0.1$ and 0.4 glasses can be satisfactorily fitted with a single Gaussian–Lorentzian peak centered at ~517.2 eV and having FHMW ~2.0 eV indicating that no V^{4+} ions are present beyond the 5% detection limit of the technique. Similar quantitative fits are found for the other two glass compositions. The results of the fitting are summarized in Table 4.

As was mentioned earlier, it was found in previous studies that Te [19] ions exist in TeO_4 tbp and TeO_3 tp environments in vanadium tellurite glass samples with similar composition to the one studied here. We, therefore, tried to fit the Te $3d_{5/2}$ core level spectra with two contributions, one due to Te ions in TeO_4 environment at a BE of ~577 eV with a FWHM of ~1.9 EV and the other due to Te ions in TeO_3 environment at a BE of ~576 eV with a FWHM of ~1.9 eV. Fig. 6 shows such a fitting for the glass composition $x = 0.3$ and $x = 0.4$. Similar fitting was performed on the other two samples and the results are displayed in Table 5. We see from the table that

Table 4
Peak positions, FWHM, and relative concentration of V^{4+} resulting from the curve fittings of the V 2p spectra for the xV_2O_5–$(1-x)TeO_2$ glasses.

x	V $2p_{3/2}$		$[V^{4+}]/[V_{total}]$[a]
	Position (eV)	FWHM (eV)	
0.10	517.1	2.0	0
0.20	517.1	2.0	0
0.30	517.2	1.8	0
0.40	517.3	1.8	0

The experimental uncertainty is ±0.2 eV in the energy measurement.
[a] If there are any V^{4+} ions, their content is beyond the detection limit of the XPS technique.

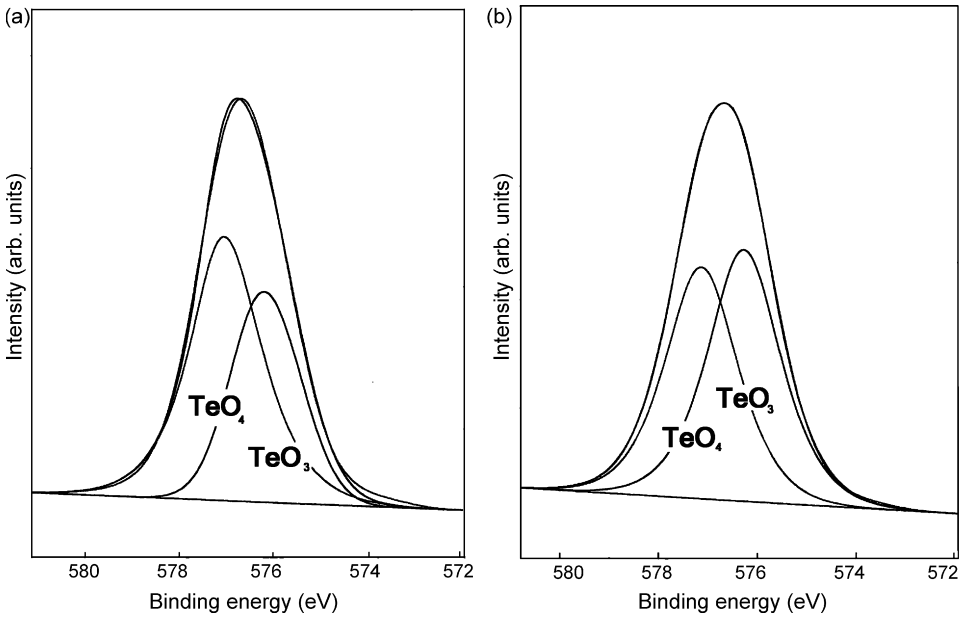

Fig. 6. Te $3d_{5/2}$ core level spectra fitted with two contributions, one due to TeO_4 tbp configuration and the other due to TeO_3 tp configuration for (a) $x = 0.3$ and (b) $x = 0.4$ glass compositions.

Table 5
Peak positions, area, FWHM, peak separation, and relative concentration of TeO_3 resulting from the curve fittings of the Te $3d_{5/2}$ spectra for the xV_2O_5–$(1-x)TeO_2$ glasses.

x	Te $3d_{5/2}$ (TeO_3)			Te $3d_{5/2}$ (TeO_4)			ΔE (eV)	[TeO_3] %
	Position (eV)	FWHM (eV)	Area	Position (eV)	FWHM (eV)	Area		
0.10	575.7	1.86	4,524	576.7	2.00	18,751	1.0	19
0.20	575.7	1.90	12,799	576.7	1.85	29,030	1.0	31
0.30	576.1	1.75	8,060	577.1	1.85	11,381	1.0	41
0.40	576.3	1.80	31,712	577.3	1.80	28,798	1.0	52

The experimental uncertainty is ±0.2 eV in the energy measurement and ±10% in the relative concentration of TeO_3.

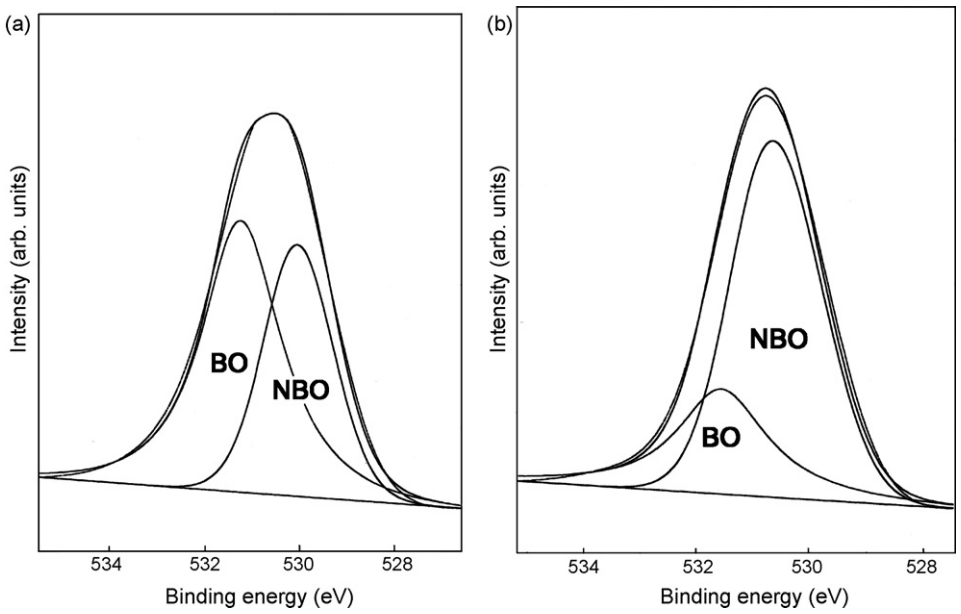

Fig. 7. O 1s core level spectra fitted with BO and NBO peaks for (a) $x = 0.1$ and (b) $x = 0.4$ glass compositions.

substituting V_2O_5 for TeO_2 increases the TeO_3 content in the glasses from ~20% at the lowest V_2O_5 content to ~50% at the highest V_2O_5 content. These values are in reasonably good agreement with those found using NMR [18] and neutron diffraction [19].

Among the most informative XPS spectra in glasses are those related to the oxygen atoms, namely of the O 1s spectra. The XPS technique has been successfully used to determine the proportions of bridging oxygen atoms (BO) and non-bridging oxygen atoms (NBO) in various glass systems. It has been used in simple binary glasses as well as ternary glass systems. Correspondingly, the O 1s peaks for these V_2O_5–TeO_2 glasses may arise from oxygen atoms existing in some or all of the following structural units: Te–O–Te, Te–O–V, V–O–V, and V=O. Oxygen atoms that are covalently bonded to glass former atoms on both sides are typically called bridging oxygen (e.g., P–O–P, Si–O–Si, Ge–O–Ge), while oxygen atoms ionically bonded, at least on one side, or double bonded to a glass former atom are referred to as non-bridging oxygens and have lower binding energies (e.g., Si–O–Na, Ge–O–Na, V=O, P=O). As described in the previous section, the O 1s peaks for the V_2O_5–TeO_2 glass samples exhibit an asymmetry and correspondingly the O 1s spectra were fitted to two Gaussian–Lorentzian peaks as shown in Fig. 7. The resulting relative abundance of NBO/O_{total} (see Table 6) increased from 43% to 76% as the nominal V_2O_5 content increased from 0.1 to 0.4. However since the abundance of the V–O–V and V–O–Te structures should increase with increasing V_2O_5 content, the oxygen atoms in V–O–V and V–O–Te structures in these glasses are more likely to be associated with non-bridging oxygens (NBO) rather than BO atoms in order to account for the observed increase in the relative abundance of NBO. Furthermore, each TeO_3 unit introduced in the glass structure contributes 2 NBOs [19]. The NBO content introduced from TeO_4 units through the $O_{3/2}Te–O^-$ structure are taken from Table 5 of Ref. [18]. Assuming that all V atoms in V_2O_5 give rise to an NBO [21], the total number of NBOs in each glass composition would be given by:

$$\frac{\text{NBO}}{\text{TO}} = \frac{5x + 2(1-x)[\text{TeO}_3] + y[\text{TeO}_4]}{2 + 3x} \quad (1)$$

Table 6
Peak positions, area, FWHM, peak separation, and relative concentration of NBO resulting from the curve fitting of the O 1s core level for the xV_2O_5–$(1-x)TeO_2$ glasses.

x	O 1s (eV)		FWHM (eV)		ΔE_{BO-NBO} (eV)	[NBO] %	
	NBO (area)	BO (area)	NBO	BO		Measured	Cal[a]
0.10	530.0 (3147)	531.2 (4248)	1.90	2.00	1.2	43	40
0.20	530.0 (7451)	531.2 (7892)	2.00	2.00	1.2	49	60
0.30	530.3 (5292)	531.3 (2630)	1.85	1.85	1.0	67	80
0.40	530.5 (25,624)	531.5 (7976)	1.90	1.90	1.0	76	

The experimental uncertainty is ±0.2 eV in the energy measurement and ±10% in the relative concentration of NBO.
[a] Calculated using Eq. (1).

where the actual values of x as determined from ICP (Table 1) were used in Eq. (1) and [TeO_3] and [TeO_4] are the concentrations of TeO_3 and TeO_4 structural units in the glass determined from XPS (Table 5). Each V_2O_5 molecule would contribute five NBO atoms to the O 1s peak, each TeO_3 structural unit would result in 2 NBOs while the contribution of TeO_4 to the NBOs is taken from Table 5 of Ref. [18]. The qualitative agreement between the values of NBO/O_{total} determined from the relative areas under the O 1s peaks are displayed in Table 6 and the corresponding values calculated from Eq. (1) strongly supports this conjecture that the oxygen atoms in V–O–V and V–O–Te are probably more non-bridging in character compared to those in Te–O–Te units. Moreover, these rather large relative abundances of NBO indicate that V_2O_5 plays the role of a network modifier rather than a glass former in this glass system in a similar way it did in the vanadium phosphate glasses investigated by the same group [21]. We can in general state that V_2O_5 can be considered as both a glass former and modifier.

5. Conclusions

XPS and magnetization studies were performed to investigate the effect of substituting various amounts of V_2O_5 for TeO_2 in a V_2O_5–TeO_2 binary glass system. The XPS analysis of the Te $3d_{5/2}$ core level indicated the existence of Both TeO_4 and TeO_3 and that the fraction of TeO_3 increases with increasing V_2O_5 content in agreement with previous studies conducted on the same glass system. The O 1s spectra with a conventional two-peak fit and the number of NBO in each glass was found to correspond to contributions from V–O–V, V–O–Te, V═O and TeO_3 and some of the TeO_4 structural units. The V 2p spectra were fitted with a single peak corresponding to V^{5+} ions. The magnetic susceptibility data for these glasses follow a Curie–Weiss behavior which also indicates the presence of some V ions existing in a magnetic state V^{4+} in addition to the presence of the non-magnetic state V^{5+}. This ~3.5% presence of V ions in V^{4+} state is beyond the 5% detection limit of XPS.

Acknowledgments

Two of the authors (AM) and (GDK) would like to acknowledge the support of the Physics Department at KFUPM.

References

[1] N. Uchida, K. Takahashi, K. Nakata, S. Shibusawa, Yogyo Kyokai Shi 86 (1978) 317.
[2] T. Yoko, K. Kamiya, K. Tanaka, H. Yamada, S. Sakka, Nippon Seramikkusu Kyokai Gakujutsu Ronbunshi 97 (1989) 289.
[3] J. Heo, D. Lam, G.H. Sigel Jr., E.A. Mendoza, D.A. Hensley, J. Am. Ceram. Soc. 75 (1992) 277.
[4] T. Sekiya, N. Mchida, A. Ohtsuka, M. Tonokawa, Nippon Seramikkusu Kyokai Gakujutsu Ronbunshi 97 (1989) 1435.
[5] T. Sekiya, N. Mchida, A. Ohtsuka, M. Tonokawa, J. Non-Cryst. Solids 144 (1992) 128.
[6] Y. Himei, A. Osaka, T. Nanba, Y. Miura, J. Non-Cryst. Solids 177 (1994) 164.
[7] M. Tastumisago, T. Minami, Y. Kowada, H. Adachi, Phys. Chem. Glasses 35 (1994) 89.
[8] T. Yoko, M. Fujita, F. Miyaji, S. Sakka, Chem. Expr. 5 (1990) 549.
[9] A. Osaka, Q. Jianrong, T. Nanba, Y. Miura, T. Yao, J. Non-Cryst. Solids 142 (1992) 81.
[10] H. Yamamoto, H. Nasu, J. Matsuoka, K. Kamiya, J. Non-Cryst. Solids 170 (1994) 87.
[11] Y. Shimizugawa, T. Maeseto, S. Suehara, S. Inoue, A. Nukui, J. Mater. Res. 10 (1995) 405.
[12] G.W. Brady, J. Chem. Phys. 27 (1957) 300.
[13] S. Neov, V. Kozhukharov, I. Gerasimova, K. Krezhov, B. Sidzhimov, J. Phys. C: Solid State Phys. 12 (1979) 2475.
[14] K. Suzuki, J. Non-Cryst. Solids 95–96 (1987) 15.
[15] S. Neov, I. Gerasimova, K. Krezhov, B. Sidzhimov, V. Kozhukharov, Phys. Status Solidi A 47 (1978) 743.
[16] Y. Dimitriev, V. Dimitrov, M. Arnaudov, J. Mater. Sci. 18 (1983) 1353.
[17] R.N. Sinclair, A.C. Wright, B. Bachra, Y.B. Dimitriev, V.V. Dimitrov, M.G. Arnaudov, J. Non-Cryst. Solids 232–234 (1998) 38.
[18] S. Sakida, S. Hayakawa, T. Yoko, J. Phys.: Condens. Matter 12 (2000) 2579.
[19] U. Hoppe, E. Yousef, C. Russel, J. Neuefeind, A.C. Hannon, Solid Sate Commun. 123 (2002) 273.
[20] A. Mekki, D. Holland, Kh.A. Ziq, C.F. McConville, J. Non-Cryst. Solids 272 (2000) 179.
[21] G.D. Khattak, A. Mekki, L.E. Wenger, J. Non-Cryst. Solids, in press.